

A MEASUREMENT OF DISK ELLIPTICITY IN NEARBY SPIRAL GALAXIES

DAVID R. ANDERSEN

Department of Astronomy and Astrophysics, Pennsylvania State University, 525 Davey Laboratory,
University Park, PA 16802; andersen@astro.psu.edu

AND

MATTHEW A. BERSHADY, LINDA S. SPARKE, JOHN S. GALLAGHER III, AND ERIC M. WILCOTS

Department of Astronomy, University of Wisconsin at Madison, 475 North Charter Street, Madison, WI 53706;
mab@astro.wisc.edu, sparke@astro.wisc.edu, jsg@astro.wisc.edu, ewilcots@astro.wisc.edu

Received 2000 September 22; accepted 2001 March 6; published 2001 April 6

ABSTRACT

We have measured the intrinsic disk ellipticity for seven nearby, nearly face-on spiral galaxies by combining Densepak integral-field spectroscopy with *I*-band imaging from the WIYN telescope. Initially assuming an axisymmetric model, we determine the kinematic inclinations and position angles from H α velocity fields and the photometric axis ratios and position angles from imaging data. We interpret the observed disparities between kinematic and photometric disk parameters in terms of an intrinsic nonzero ellipticity ϵ . The mean ellipticity of our sample is 0.05. If the majority of disk galaxies have such intrinsic axis ratios, this would account for roughly 50% of the scatter in the Tully-Fisher relation. This result, in turn, places tighter constraints on other sources of scatter in this relation, the most astrophysically compelling of which is galaxy mass-to-light ratios.

Subject headings: galaxies: kinematics and dynamics — galaxies: structure

1. INTRODUCTION

A large fraction of galaxy disks appears to be nonaxisymmetric. Photometric studies of face-on galaxies find that the light distribution in 30%–50% of spiral galaxies is lopsided ($m = 1$ distortions; Zaritsky & Rix 1997; Rudnick & Rix 1998) or has higher order distortions ($m \geq 2$; Rix & Zaritsky 1995; Kornreich, Haynes, & Lovelace 1998; Conselice, Bershad, & Jangren 2000). A similar fraction of galaxies has lopsided H I distributions or kinematic asymmetries (Baldwin, Lynden-Bell, & Sancisi 1980; Bosma 1981; Richter & Sancisi 1994; Haynes et al. 1998; Swaters et al. 1999).

Disk ellipticity ($m = 2$) may also be common. Few disk galaxies appear round on the sky; the distribution of apparent axis ratios is best modeled by randomly oriented disks with intrinsic ellipticities $\epsilon \sim 0.1$ (Binney & de Vaucouleurs 1981; Grøsbol 1985; Huizinga & van Albada 1992; Lambas, Maddox, & Loveday 1992). These statistical studies constrain mean ellipticity but do not probe the intrinsic ellipticity of individual galaxies.

If galaxy disks are elongated, errors in photometric estimates of inclinations and position angles (P.A.'s) will be introduced, thereby contributing to the scatter in the relationship between galaxy luminosity and rotation speed (Tully & Fisher 1977). Franx & de Zeeuw (1992) used a specific, nonrotating velocity field model to show that if $\epsilon = 0.1$ on average, systematic errors could account for all the observed scatter in the Tully-Fisher (TF) relation. However, the true contribution to this scatter depends on the distribution of intrinsic axis ratios. Identifying the individual ellipticities of galaxies would limit other sources of astrophysical scatter in the TF relation and reduce scatter.

Kinematic maps can be used to estimate ellipticity for individual galaxy disks. One approach involves fitting such maps with elliptic orbits, from which a quantity related to the ellipticity of the potential can be estimated: $\epsilon_{\text{pot}} \sin 2\phi$. This quantity varies from 0.001 to 0.07 for a sample of nine galaxies (Schoenmakers, Franx, & de Zeeuw 1997; Schoenmakers 1999). Unfortunately, the phase angle ϕ is not directly measurable. Such

studies have been rare because they require observationally expensive, high-resolution, high signal-to-noise ratio velocity field maps (e.g., Teuben et al. 1986; Kornreich et al. 2000).

Here we develop a new, efficient method of estimating intrinsic galaxy disk ellipticities using optical kinematic maps and photometric indices. Determining unique solutions for ϵ and ϕ requires measurements of both kinematic and photometric inclination and P.A.'s for nearly face-on spiral disks. When the disk major axis is rotated by a phase angle ϕ away from the line of nodes, the kinematic and photometric axes will appear misaligned only if $\cos i < 1 - \epsilon$. If $\epsilon \approx 0.1$, as suggested by earlier studies, substantial misalignment of kinematic and photometric P.A.'s ($>30^\circ$) will occur only for galaxies with $i < 30^\circ$. To demonstrate our method, we present the detailed analysis of WIYN¹ integral-field H α velocity fields and *I*-band images for UGC 4380 and measurements of ϵ for an additional six, nearly face-on galaxies based on the same method.

2. SAMPLE AND OBSERVATIONS

Our sample of seven galaxies is a subset of 69 selected from the Principal Galaxy Catalog (Paturel et al. 1997) in regions of low Galactic extinction with normal surface brightnesses, axis ratios corresponding to less than 30° inclination for a circular disk, diameters D_{25} between 0'.75 and 1'.5 (to facilitate spectroscopic follow-up), and Hubble types between Sb and Sc (D. R. Andersen, M. A. Bershad, L. Sparke, J. Gallagher, E. Wilcots, W. van Driel, & D. Ragaigine 2001, in preparation). We excluded galaxies with obvious bars, clearly visible non-axisymmetric structure, and foreground stars within 2–4 disk scale lengths using the Second Palomar Observatory Sky Survey.

We used the WIYN S2KB imager (a 2048² CCD with 0'.195 pixel⁻¹) to obtain deep *I*-band images of our seven targets between 1999 May 10 and 14 with seeing of $\sim 1''.1$ FWHM, or

¹ The WIYN Observatory is a joint facility of the University of Wisconsin–Madison, Indiana University, Yale University, and the National Optical Astronomy Observatories.

10% of 1 scale length. We reduced these images using standard procedures, yielding a sufficient signal-to-noise ratio to establish galaxy isophotes to ~ 4.5 scale lengths. We used flux-calibrated, R -band magnitudes obtained with the IGI/TK4 imager on the McDonald Observatory 107" telescope to check that these galaxies had close to "Freeman" disks (a B -band central disk surface brightness of $21.7 \text{ mag arcsec}^{-2}$). For example, assuming $B-R = 1.15$ for the Sc-type galaxy UGC 4380, we find that $\mu_0(B) = 21.5 \text{ mag arcsec}^{-2}$.

Spectral images of our seven targets were obtained using Densapak on the WIYN telescope from portions of runs on 1998 May 20–21, 1999 January 20–22, and 1999 March 27–28. Densapak is a fiber-optic array used for integral-field spectroscopy containing 86 active, $3''$ fibers (separated by $4''$) arranged in a 7×13 staggered grid subtending an area of $30'' \times 45''$ (Barden, Sawyer, & Honeycutt 1998). Four additional "sky" fibers are spaced around this grid roughly $1'$ from the grid center. Densapak feeds the WIYN Bench Spectrograph, which we used with an echelle grating to cover $6600 \text{ \AA} < \lambda < 7000 \text{ \AA}$ with a dispersion of $0.19 \text{ \AA pixel}^{-1}$ and an FWHM spectral resolution of 0.51 \AA . Basic spectral reductions were done using the NOAO IRAF package DOHYDRA. Thorium-argon lamps were used for wavelength calibration.

Since galaxy rotation curves peak at roughly 2 photometric scale lengths (Courteau & Rix 1999; Willick 1999), we used Densapak to map out to ~ 3 scale lengths per galaxy (typically $\sim 30''$). For UGC 4380, which has an I -band scale length of $9''.7$, two Densapak pointings were required to cover a square of roughly $45 \times 45 \text{ arcsec}^2$. Two 30 minute exposures were made at each Densapak position to facilitate cosmic-ray removal. The $H\alpha$ line flux was typically measured at a signal-to-noise ratio of ~ 10 at the edge of our observed field.

3. MEASUREMENTS

To measure photometric axis ratios and P.A.'s, we use the STSDAS ISOPHOTE package ELLIPSE on images with stars masked. Figure 1 shows the radial dependence of P.A., apparent ellipticity ($1 - b/a$), and an azimuthal variance statistic for UGC 4380. Inside $29''$, the variance statistic is greater than unity, showing that spiral-arm structure affects the ellipse fits. Hence, we measure the photometric axis ratio and P.A. at radii greater than $29''$, where the axis ratio and P.A. are constant, consistent with our estimate that spiral structure has a minimal impact.

To determine kinematic inclination and P.A.'s, we first produce $H\alpha$ emission-line maps from the 86 field-flattened and sky-subtracted spectra from each pointing. We measure velocity centroids by fitting a Gaussian line profile to each $H\alpha$ line, and we assign a spatial position based on the fiber geometry of Densapak and the offsets used to make multiple pointings. Figure 2 shows a polynomial surface fit to these discrete velocity measurements for UGC 4380. UGC 4380 clearly is an inclined galaxy with a center coincident with the photometric center. The formally well-determined P.A. and peak rotation velocity (Table 1) agree with the visual inspection of the data (Fig. 2). Single-dish $H\text{ I}$ observations of UGC 4380 list a W_{50} velocity width of 118 km s^{-1} (Haynes et al. 1988). The W_{50} width measured from our Densapak spectra is also 118 km s^{-1} , implying we observed the peak of the rotation curve.

To extract the P.A., peak velocity, and inclination, we fitted the velocities expected at each fiber position using a simple model consisting of concentric and coplanar circular orbits with $V(r) = V_c \tanh(r/h)$, where the terminal circular velocity V_c and

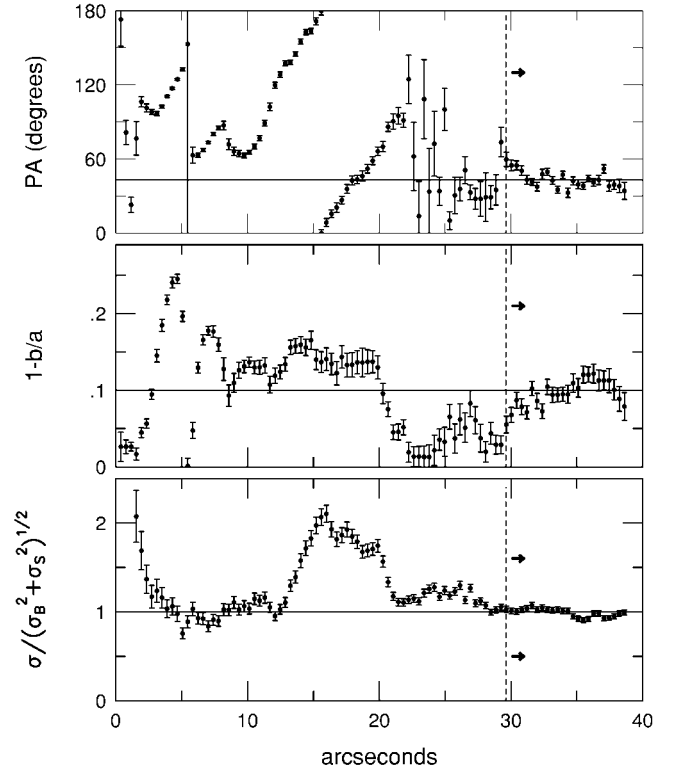


FIG. 1.—Radial dependencies of photometric P.A. (top panel) and ellipticity ($1 - b/a$; middle panel) of UGC 4380's I -band isophotes. The bottom panel shows the azimuthal surface brightness variance around each isophotal ellipse, normalized by the expected shot noise (source noise σ_s and sky plus read noise σ_b). This normalized variance is large (>1) where the spiral structure contributes to the overall variance budget. We measure the P.A. and b/a between $29''$ and $39''$, where both the P.A. and axis ratio remain constant, the azimuthal surface brightness variance is consistent with the shot noise, and the signal-to-noise ratio per pixel is greater than 1.

h are free parameters. The other free variables are the inclination, P.A., center, and central velocity. Our velocity fields exhibit only small deviations from this simple model, as illustrated for UGC 4380 in the middle panel of Figure 2. The best-fitting model was determined from χ^2 minimization (downhill simplex method) based on comparing the measured velocity centroids, fiber by fiber, with the smooth model velocity field sampled with the Densapak footprint. The standard deviation in the fit residuals is 4.3 km s^{-1} . More elaborate radial velocity functions do not provide smaller residuals yet have more independent variables. Formal confidence limits (CLs) were placed on these quantities by determining surfaces of constant χ^2 . Table 1 contains our measurements of the axis ratio, photometric P.A., and kinematic inclination and P.A. In UGC 4380, the photometric and kinematic P.A.'s differ by 9.5 ± 3.9 (68% CLs). This disk is unlikely to be intrinsically circular.

4. ANALYSIS AND RESULTS

We can estimate the ellipticity required to produce the above level of discrepancy by modeling the observed galaxy as a disk with intrinsic, photometric ellipticity ϵ (Fig. 2, right panel) but circular orbits (justified below). The vector describing the ellipse in the galaxy plane is $r' = [-(1 - \epsilon) \sin \theta, \cos \theta]$, where $\theta = 0$ is the major axis. To project the ellipse onto the (observed) sky plane, it is inclined by an angle i about the line of nodes at an angle ϕ from the intrinsic major axis. In the

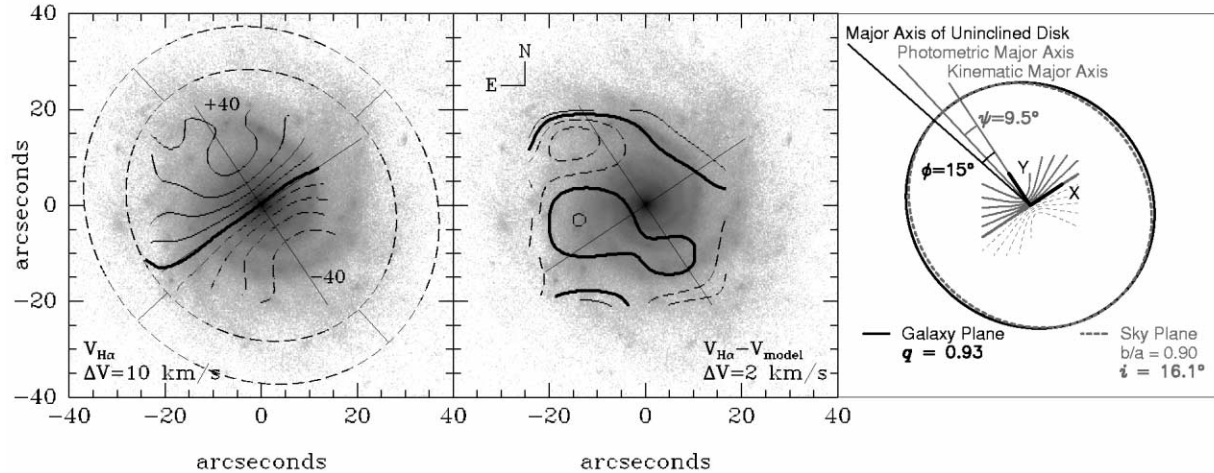


FIG. 2.—Densepak $H\alpha$ velocity field of UGC 4380 (*left panel*) and the residuals between the velocity field and a simple model (*middle panel*; see text). Both are smoothed and interpolated using a polynomial surface. Solid, thick, and dashed lines are positive, zero, and negative velocities, respectively, relative to the model systemic velocity (*left panel*) or model velocity field (*middle panel*). The dash-dotted lines (*left panel*) represent the isophotal annulus determined from Fig. 1 from which the photometric b/a and P.A. are derived (solid lines in annulus indicate photometric major and minor axes). The right, summary panel shows a schematic diagram of an isophote for UGC 4380 assuming its disk has an intrinsic ellipticity of $\epsilon = 0.07$. The x - y plane has been rotated $33^\circ 5'$ from the north to match the kinematic P.A. of UGC 4380. The solid ellipse represents the true shape of the disk seen face-on; the major axis lies at an angle $\phi = 15^\circ$ from the line of nodes (the kinematic major or y -axis). The dashed ellipse represents the apparent shape after inclining the elliptic disk by $i = 16^\circ 1'$; it has an apparent axis ratio of $b/a = 0.90$. The kinematic and photometric P.A.'s differ by $\psi = 9^\circ 5'$.

plane of the sky, the ellipse describing the galaxy isophotes is given by a transformation matrix involving θ , i , ϵ , and ϕ .

Franx & de Zeeuw (1992) found that for orbits in a flat but elliptic disk, fitting the velocity field with tilted circular rings yields the correct disk orientation to first order in ellipticity. Accordingly, we take the kinematic inclination and P.A. to represent the true inclination and P.A. of the disk; ϵ and ϕ can then be determined given measurements of the apparent photometric axis ratio (b/a), the kinematic inclination (i), and the difference between photometric and kinematic P.A.'s (ψ).

When the true inclination i is closer to face-on than the photometric inclination, as is the case for UGC 4380, the galaxy must be at least as flattened as $\epsilon \geq 1 - b/a \sec i$. The intrinsic flattening must be even larger if the true major axis does not lie in the plane of the sky. This lower limit for UGC 4380, $\epsilon > 0.06 \pm 0.03$, is inconsistent with a purely circular disk. By utilizing the $9^\circ 5' \pm 3^\circ 9'$ misalignment of the photometric and kinematic P.A.'s, a better estimate of the ellipticity can be obtained.

In general, three equations relate the three observables b/a , i , and ψ to the three unknowns ϵ , ϕ , and the angle θ at the apparent major axis. Using the Newton-Raphson method for nonlinear equations, we find that $\epsilon = 0.07^{+0.08}_{-0.06}$ (99% CLs) for UGC 4380, a solution *inconsistent* with a circular disk. Derived

values for the seven galaxies, plotted in Figure 3 and listed in Table 1, range from $\epsilon = 0.02$ to 0.20. Three galaxies (UGC 4380, NGC 2794, and UGC 5274) are inconsistent with having circular disks at the 99% CLs; two galaxies (NGC 3890 and NGC 5123) have ellipticities inconsistent with circular disks at the 95% CLs. Only two galaxies (UGC 7208 and UGC 10436) are consistent with having circular disks within their 68% CLs. The galaxies with the highest derived ellipticity ϵ have ϕ near 90° ; the line of nodes is almost perpendicular to the true major axis. This is consistent with our selection of round, apparently face-on systems. The two galaxies with $\epsilon > 0.1$, NGC 2794 and UGC 5274, both show evidence of faint, interacting companions; NGC 2794 has an active galactic nucleus.

Finally, we have checked that potential sources of systematic errors—lopsidedness, spiral structure, and warps—do *not* affect our ellipticity measurements appreciably. Table 1 contains the $\langle A_1 \rangle$ amplitude of the $m = 1$ component of the Fourier expansion of the light profile as defined by Zaritsky & Rix (1997). With the exception of NGC 5123, these galaxies are not significantly lopsided ($\langle A_1 \rangle < 0.2$), nor does $\langle A_1 \rangle$ correlate with our derived values for ψ or ϵ . None of these galaxies show any sign of kinematic asymmetry. A 180° rotational asymmetry measure, defined as $A_{180} = |\sum (V_{\text{obs}} + V_{180})| / |2 \sum V_{\text{obs}}|$, akin to

TABLE 1
PHOTOMETRIC AND KINEMATIC PROPERTIES

Identification	b/a	P.A. _{phot} (deg)	i_{kin} (deg)	P.A. _{kin} (deg)	ψ (deg)	ϕ (deg)	ϵ	ϵ CLs			$\langle A_1 \rangle$
								68%	95%	99%	
UGC 4380	0.90 ± 0.02	43 ± 4	16.1 ± 2.3	33.5 ± 1.8	10 ± 9	15 ± 15	0.07	+0.04 -0.04	+0.06 -0.06	+0.08 -0.06	0.06 ± 0.02
NGC 2794	0.85 ± 0.04	408 ± 3	20.5 ± 1.4	327.9 ± 0.9	80 ± 3	83 ± 4	0.20	+0.07 -0.07	+0.11 -0.11	+0.13 -0.13	0.04 ± 0.02
UGC 5274	0.94 ± 0.02	78 ± 7	32.2 ± 3.8	9.5 ± 1.4	69 ± 7	84 ± 5	0.20	+0.07 -0.06	+0.12 -0.10	+0.14 -0.11	0.07 ± 0.02
NGC 3890	0.96 ± 0.02	264 ± 16	23.5 ± 1.8	225.6 ± 1.4	38 ± 16	73 ± 13	0.08	+0.05 -0.04	+0.07 -0.07	+0.08 -0.08	0.13 ± 0.06
UGC 7208	0.94 ± 0.01	325 ± 9	23.8 ± 2.3	330.4 ± 1.2	-5.4 ± 9	101 ± 90	0.03	+0.04 -0.03	+0.06 -0.03	+0.08 -0.03	0.12 ± 0.05
NGC 5123	0.92 ± 0.01	163 ± 4	22.2 ± 1.1	153.0 ± 0.5	10 ± 4	44 ± 27	0.03	+0.02 -0.02	+0.04 -0.03	+0.04 -0.03	0.25 ± 0.10
UGC 10436	0.87 ± 0.03	270 ± 3	30.6 ± 1.4	267.1 ± 0.7	3 ± 3	64 ± 90	0.02	+0.06 -0.02	+0.09 -0.02	+0.11 -0.02	0.09 ± 0.05

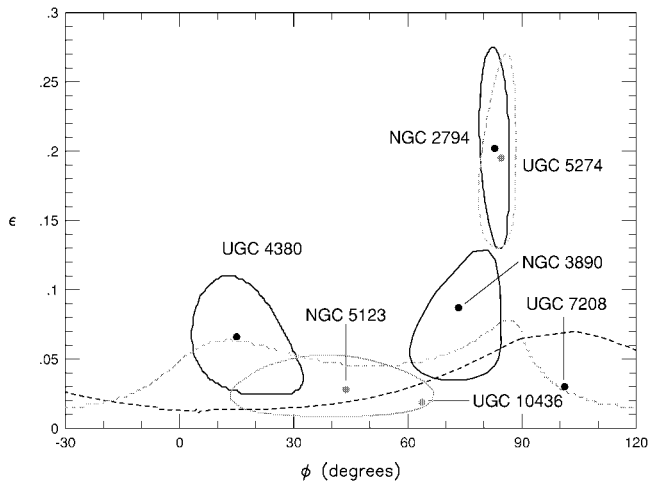


FIG. 3.—Solutions for ellipticity ϵ and angle ϕ for seven sample galaxies. The 68% CLs, shown as contours, are derived from the estimated measurement errors on b/a , ψ , and i listed in Table 1. UGC 7208 (dark-dashed line) and UGC 10436 (light-dashed line) are consistent with a circular disk within the 68% CLs.

the photometric asymmetry parameter of Conselice et al. (2000), yields close to null values for all.

Strong spiral structure drives photometric P.A.'s to change with radius R at a rate of $\partial \text{P.A.} / \partial \log R = \cot \theta_p$, where θ_p is the pitch angle of the arms. A warp in the disk also would manifest as a twisting P.A. with radius. As discussed in § 3, we make our photometric measurements between 3 and 4 scale lengths, where we find that the photometric P.A. and axis ratio are constant, and our azimuthal variance statistic (Fig. 1) corroborates that spiral structure is no longer a dominant photometric effect. The velocity fields exhibit no residual structure correlating with radius or azimuth, despite the fact that these measurements are *within* 3 scale lengths (in contrast to our photometric measurements). We find no evidence for twisting P.A.'s in the velocity fields, which is not surprising since even galaxies with strong outer warps usually have planar H I distributions within 3 scale lengths (Briggs 1990).

Baldwin, J. E., Lynden-Bell, D., & Sancisi, R. 1980, MNRAS, 193, 313
 Barden, S. C., Sawyer, D. G., & Honeycutt, R. K. 1998, Proc. SPIE, 3355, 892
 Binney, J., & de Vaucouleurs, G. 1981, MNRAS, 194, 679
 Bosma, A. 1981, AJ, 86, 1825
 Briggs, F. H. 1990, ApJ, 352, 15
 Conselice, C. J., Bershad, M. A., & Jangren, A. 2000, ApJ, 529, 886
 Courteau, S., & Rix, H. W. 1999, ApJ, 513, 561
 Franx, M., & de Zeeuw, T. 1992, ApJ, 392, L47
 Grøsbol, P. J. 1985, A&AS, 60, 261
 Haynes, M. P., Magri, C., Giovanelli, R., & Starosta, B. M. 1988, AJ, 95, 607
 Haynes, M. P., van Zee, L., Hogg, D. E., Roberts, M. S., & Maddalena, R. J. 1998, AJ, 115, 62
 Huizinga, J. E., & van Albada, T. S. 1992, MNRAS, 254, 677
 Kornreich, D. A., Haynes, M. P., & Lovelace, R. V. E. 1998, AJ, 116, 2154
 Kornreich, D. A., Haynes, M. P., Lovelace, R. V. E., & van Zee, L. 2000, AJ, 120, 139

5. SUMMARY AND DISCUSSION

We have demonstrated that high-quality H α velocity maps and I -band images of nearly face-on galaxies can be used to *exclude the hypothesis that galaxy disks are intrinsically free of $m = 2$ (elliptic) distortions*. Our method for estimating the deviation from circularity suggests that UGC 4380 has an intrinsic ellipticity of $\sim 7\%$. This is one of the first unambiguous detections of disk ellipticity for an individual galaxy. If disks are intrinsically elliptic, the photometric and kinematic axes will be misaligned in general, and the inclinations derived from isophote shapes will differ from the kinematic inclinations. Deviations are particularly large for face-on galaxies. WIYN/Densepak echelle spectroscopy and optical imaging are efficient means to estimate disk ellipticity for large samples of such systems.

The intrinsic ellipticity for our seven galaxies is $\epsilon = 0.05 \pm 0.01$ (error-weighted mean and uncertainty), inconsistent with purely circular disks. Most of our targets are normal, intermediate-type spiral galaxies, typical of those selected for TF surveys. According to Franx & de Zeeuw (1992), $\epsilon = 0.05$ should produce $\sim 50\%$ of the observed TF scatter in red and near-infrared bands. The cause of disk ellipticity is currently unclear; e.g., halo triaxiality or nonuniform matter accretion could be responsible. If larger samples show disk ellipticity at these levels, this implies that variations in either the disk mass fractions or the mass-to-light ratio of today's spiral galaxies must contribute under 0.1–0.2 mag of dispersion in the luminosity of galaxies at a given rotation speed. High-resolution cosmological simulations (e.g., Steinmetz & Navarro 1999; van den Bosch 2000) indicate that variance in disk mass fraction should only induce scatter *along* the TF relation because halo contraction is greater for larger disk masses. Assuming the remaining scatter in the observed TF relation is dominated by differences in spiral galaxy mass-to-light ratios, this modest variance places strong constraints on the formation histories of such systems.

We thank S. Barden and D. Sawyer for making Densepak happen. This research was supported by the UW-Madison Graduate School and NSF grants AST 96-18849 and AST 99-70780 (M. A. B.).

REFERENCES

Lambas, D. G., Maddox, S. J., & Loveday, J. 1992, MNRAS, 258, 404
 Paturel, G., et al. 1997, A&AS, 124, 109
 Richter, O. G., & Sancisi, R. 1994, A&A, 290, L9
 Rix, H. W., & Zaritsky, D. 1995, ApJ, 447, 82
 Rudnick, G., & Rix, H. W. 1998, AJ, 116, 1163
 Schoenmakers, R. H. M. 1999, Ph.D. thesis, Rijkuniversiteit Groningen
 Schoenmakers, R. H. M., Franx, M., & de Zeeuw, P. T. 1997, MNRAS, 292, 349
 Steinmetz, M., & Navarro, J. F. 1999, ApJ, 513, 555
 Swaters, R. A., Schoenmakers, R. H. M., Sancisi, R., & van Albada, T. S. 1999, MNRAS, 304, 330
 Teuben, P. J., Sanders, R. H., Atherton, P. D., & van Albada, G. D. 1986, MNRAS, 221, 1
 Tully, R. B., & Fisher, J. R. 1977, A&A, 54, 661
 van den Bosch, F. C. 2000, ApJ, 530, 177
 Willick, J. A. 1999, ApJ, 516, 47
 Zaritsky, D., & Rix, H. W. 1997, ApJ, 477, 118